



Effect of the dipeptidyl peptidase-4 inhibitor linagliptin on atherosclerotic lesions in Watanabe heritable hyperlipidemic rabbits: iMap-IVUS and pathological analysis

Takafumi Kurosawa¹ · Yuxin Li² · Mitsumasa Sudo¹ · Hironori Haruta¹ · Kazuhiro Hagikura² · Tadateru Takayama¹ · Takafumi Hiro¹ · Masashi Shiomi³ · Hiroyuki Hao⁴ · Taro Matsumoto² · Atsushi Hirayama¹ · Yasuo Okumura¹

Received: 16 April 2020 / Accepted: 28 August 2020 / Published online: 10 September 2020
© Springer Japan KK, part of Springer Nature 2020

Abstract

Dipeptidyl peptidase-4 (DPP-4) inhibitors have potential as a treatment for atherosclerosis. However, it is unclear whether DPP-4 inhibitors stabilize atherosclerotic plaque or alter the composition of complex plaque. Sixteen Watanabe heritable hyperlipidemic rabbits aged 10–12 weeks with atherosclerotic plaque in the brachiocephalic artery detected by iMap™ intravascular ultrasound (IVUS) were divided into a DPP-4 inhibitor group and a control group. Linagliptin was administered to the DPP-4 inhibitor group via nasogastric tube at a dose of 10 mg/kg/day for 16 weeks, and control rabbits received the same volume of 0.5% hydroxyethylcellulose. After evaluation by IVUS at 16 weeks, the brachiocephalic arteries were harvested for pathological examination. IVUS revealed that linagliptin significantly reduced the plaque volume and vessel volume (control group vs. DPP-4 inhibitor group: Δ plaque volume, $1.02 \pm 0.96 \text{ mm}^3$ vs. $-3.59 \pm 0.92 \text{ mm}^3$, $P=0.004$; Δ vessel volume, $-1.22 \pm 2.36 \text{ mm}^3$ vs. $-8.66 \pm 2.33 \text{ mm}^3$, $P=0.04$; %change in plaque volume, $6.90 \pm 5.62\%$ vs. $-15.06 \pm 3.29\%$, $P=0.005$). With regard to plaque composition, linagliptin significantly reduced the volume of fibrotic, lipidic, and necrotic plaque (control group vs. DPP-4 inhibitor group: Δ fibrotic volume, $0.56 \pm 1.27 \text{ mm}^3$ vs. $-5.57 \pm 1.46 \text{ mm}^3$, $P=0.04$; Δ lipidic volume, $0.24 \pm 0.24 \text{ mm}^3$ vs. $-0.42 \pm 0.16 \text{ mm}^3$, $P=0.04$; Δ necrotic volume, $0.76 \pm 0.54 \text{ mm}^3$ vs. $-0.84 \pm 0.25 \text{ mm}^3$, $P=0.02$). Pathological examination did not show any significant differences in the %smooth muscle cell area or %fibrotic area, but infiltration of macrophages into plaque was reduced by linagliptin treatment (%macrophage area: $12.03\% \pm 1.51\%$ vs. $7.21 \pm 1.65\%$, $P<0.05$). These findings indicate that linagliptin inhibited plaque growth and stabilized plaque in Watanabe heritable hyperlipidemic rabbits.

Keywords Atherosclerosis · Plaque · Ultrasound · Diabetes mellitus · Dipeptidyl peptidase-4 inhibitor

Introduction

It is known that atherosclerosis progresses rapidly in patients with diabetes and is more likely to become severe [1]. In several large-scale clinical trials (ACCORD, ADVANCE, and VADT trials), strict glycemic control did not significantly reduce vascular damage in patients with type 2 diabetes [2–4]. However, development of incretin-related drugs [glucagon-like peptide 1 (GLP-1) and dipeptidyl peptidase-4 (DPP-4) inhibitors] has raised the possibility of treatment for diabetes with an anti-atherosclerotic effect and cardioprotective effect [5]. Linagliptin is a DPP-4 inhibitor that does not inhibit related enzymes, such as DPP-8 and DPP-9, and shows high selectivity for DPP-4, with the lowest half maximal inhibitory concentration (IC_{50}) among existing DPP-4

✉ Yuxin Li
li.yuxin@nihon-u.ac.jp

¹ Division of Cardiology, Department of Medicine, Nihon University School of Medicine, 30-1 Oyaguchi-kamicho, Itabashi-ku, Tokyo 173-8610, Japan

² Division of Cell Regeneration and Transplantation, Department of Functional Morphology, Nihon University School of Medicine, 30-1 Oyaguchi-kamicho, Itabashi-ku, Tokyo 173-8610, Japan

³ Institute for Experimental Animals, Kobe University Graduate School of Medicine, 7-5-1 Kusunoki-cho, Chuo-ku, Kobe, Hyogo 650-0017, Japan

⁴ Department of Pathology, Nihon University School of Medicine, 30-1 Oyaguchi-kamicho, Itabashi-ku, Tokyo 173-8610, Japan

inhibitors. Linagliptin has a xanthine skeleton and this structure allows strong inhibition of DPP-4 activity.

Oxidative stress is thought to be involved in the onset and progression of atherosclerosis [6, 7]. When linagliptin was administered for 7 days to rats with sepsis, vascular endothelial function was improved, inflammatory cell infiltration into large vessels was reduced, and expression of NADPH oxidase and inflammatory genes in the aorta was downregulated [8]. Besides its hypoglycemic effect, linagliptin may have pleiotropic effects such as antioxidant and anti-inflammatory activity. However, the changes in plaque volume and composition after administration of linagliptin have not been investigated by intravascular imaging in the setting of advanced atherosclerosis.

Therefore, the present study was performed to examine the effect of linagliptin on the volume and composition of advanced atherosclerotic plaque in myocardial infarction-prone Watanabe heritable hyperlipidemic rabbits (WHHL-MI rabbits).

Materials and methods

Animals and housing

Male WHHL-MI rabbits were obtained from the laboratory animal facility attached to Kobe University School of Medicine for use as an animal model of atherosclerosis. WHHL-MI rabbits were the first animal model reported to spontaneously develop myocardial infarction [9]. Rabbits aged 10–12 months were housed in a laboratory animal room of Nihon University Medical Research Support Center. The temperature of the room was set at 22 ± 2 °C, humidity was maintained at $65 \pm 5\%$, and the lighting time was 12 h/day (from 8 AM. to 8 PM.). The rabbits were fed 100 g/day of standard chow (CR-3: CLEA Japan, Inc., Tokyo, Japan) and had free access to tap water.

Grouping of animals

Sixteen WHHL-MI rabbits aged 10–12 months were divided into two groups, which were a linagliptin group and a control group. The linagliptin group received linagliptin at a dose of 10 mg/kg/day in 0.5% Natrosol (hydroxyethylcellulose) for 16 weeks via a stomach tube and the control group was administered Natrosol alone.

These experiments were approved by the Animal Research Committee of University and were conducted in compliance with the guidelines of the Nihon University

School of Medicine and the rules of the University for Animal Experiments and management.

IVUS procedure and analysis

IVUS imaging was performed at baseline and after 16 weeks using the same system. After induction of general anesthesia with inhalation of 3–5% sevoflurane at 4 L/min, the right femoral artery was punctured with a 22G needle and a 4Fr sheath was inserted. Then, 500 units of unfractionated heparin were administered intravenously before IVUS imaging. An ultrasound imaging system ((iLab™; Boston Scientific Corporation, Marlborough, MA, USA) with iMap function (iMap™) and an IVUS imaging catheter (Atlantis SR Pro 40-MHz Catheter; Boston Scientific Corporation, Marlborough, MA, USA) were used to capture IVUS images in the brachiocephalic artery using a coronary guide wire (ASAHI SION blue; Asahi Intecc Co. Ltd. Aichi, Japan). The IVUS catheter was withdrawn by a mechanical automatic pullback system at 0.5 mm/s.

iMap™ identifies tissue properties by a method called spectral similarity analysis. In iMAP-IVUS analysis, radiofrequency ultrasound data are processed by autoregressive modeling and matched with a database of known radiofrequency signal profiles containing the characteristics of four tissue types. All IVUS images with the radiofrequency signals were stored on DVD and were analyzed offline with the use of commercial software Echo Plaque 4.0 (INDEC Medical Systems, Los Altos, CA, USA). When the IVUS catheter was automatic withdrawn in brachiocephalic artery at 0.5 mm/s, 30 frames of gray-scale IVUS images and 1 frame of radiofrequency signal data were recorded in every second, which means 60 Gy-scale IVUS images and 2 iMAP-IVUS images per millimeter. The external elastic membrane (EEM) area and lumen area were traced. After tracing the EEM and lumen of all involved iMAP-IVUS images from the distal to the proximal direction, the software Echo Plaque 4.0 automatically calculated lesion length, lumen area and volume, vessel area and volume, plaque area and volume, plaque burden, fibrotic plaque area and volume, lipidic plaque area and volume, necrotic plaque area and volume, and calcified plaque area and volume. To compensate for the effect of various lesion lengths on the volumetric variables, length-adjusted volumetric variables were used in the study. For example, length-adjusted lumen volume was calculated as: lumen volume divided by lesion length and then multiplied the median length of target segments [10]. In iMAP-IVUS images, plaque components were displayed as green for fibrotic plaque, yellow for lipidic plaque, red for necrotic plaque, and blue for calcified plaque [11–13]. The percent

of each plaque tissue component was calculated as component area/plaque area \times 100.

Histopathological examination

After 16 weeks of treatment, following IVUS examination, the rabbits were killed and perfused with 1 L of physiological saline from a height of 150 cm, corresponding to a systolic blood pressure of about 110 mmHg. After complete removal of blood by perfusion with physiological saline, the rabbits were similarly perfused with 500 mL of 10% formalin from a height of 150 cm for fixation. After confirming that fixation was adequate, the brachiocephalic artery and the right common carotid artery were resected en bloc and fixed in 10% formalin for more than 24 h. Then, a paraffin block of the brachiocephalic artery was prepared and transverse sections with a thickness of 4–5 μ m were cut at 0.5 mm intervals from distal to proximal for pathological examination. We selected iMAP-IVUS images matched sections at the same location for following evaluations. To match the histological sections to the iMAP-IVUS images, pathological evaluation and IVUS were performed in the same segment of brachiocephalic arteries, and the distance from the bifurcation and plaque features were used to ensure that IVUS and pathological sections are in the same position. Sections were subjected to staining with hematoxylin–eosin (H–E), Masson trichrome (MT), and Elastica van Gieson (EVG) stain. The lumen, internal elastic membrane (IEM), and EEM were traced. Plaque area was calculated by subtracting the lumen area from the IEM area. The fibrous component was defined as fibrocellular tissue with dense collagen bundles sparse lipid content, while the lipid component was defined as foam cells and dispersed extracellular cholesterol crystals/lipids with little collagen. In addition, the necrotic component was defined as necrotic lesions rich in cholesterol crystals and inflammatory cells with a few collagen fibers. Finally, the calcified component was defined as tissue containing strongly stained calcium crystals [14, 15].

The macrophage infiltration area and smooth muscle cell (SMC) area were determined by immunohistochemistry according to the standard protocols, using mouse monoclonal anti-rabbit macrophage antibody (Clone RAM-11, \times 50, Dako North America Inc., Carpinteria, CA, USA) and mouse anti-rabbit smooth muscle Actin antibody (Clone 1A4, \times 50, Dako North America Inc.). After immunostaining, DAB-stained RAM-11 positive and 1A4 positive proportion were measured in intimal plaques. Following digitization of images obtained with a microscope (OLYMPUS BX51, DP Controller; Ver 3.2.2.267; Olympus Corporation, Tokyo, Japan), the area of each target tissue was automatically measured using image analysis software (Photoshop CC 2017, Adobe Systems Incorporated, San Jose, CA, USA).

Statistical analysis

Differences in discrete variables between the two groups were assessed by the Chi-square test or Fisher's exact test, as appropriate. Continuous variables were reported as the mean \pm standard error of the mean, and intergroup comparisons were performed by the unpaired Student *t* test. Within-group differences in values obtained before treatment and those obtained at 16 weeks of treatment were assessed by paired Student's *t* test. Statistical analyses were done with Excel (Microsoft Corporation, Redmond, WA, USA) and Easy R statistical software (EZR Version 1.36; Jichi Medical University Saitama Medical Center, Saitama, Japan), and statistical significance was accepted at $P < 0.05$.

Results

Body weight and laboratory data

The body weight and laboratory data are listed in Table 1. The body weight was comparable between the control group and linagliptin group at baseline and after 16 weeks of treatment (Control vs. Linagliptin: before treatment, 2.82 ± 0.08 kg vs. 2.84 ± 0.04 kg, $P = 0.81$; at 16 weeks, 2.74 ± 0.11 kg vs. 3.00 ± 0.06 kg, $P = 0.06$). There was no significant difference in the lipid profile between the two groups at baseline and after 16 weeks of treatment, including total cholesterol (Control vs. Linagliptin: before treatment, 1084.3 ± 75.5 mg/dL vs. 1081.4 ± 83.4 mg/dL, $P = 0.98$; at 16 weeks, 938.9 ± 50.1 mg/dL vs. 938.6 ± 42.0 mg/dL, $P = 0.99$), low-density lipoprotein cholesterol (Control vs. Linagliptin: before treatment, 1006.4 ± 73.8 mg/dL vs. 991.4 ± 74.1 mg/dL, $P = 0.89$; at 16 weeks, 870.7 ± 57.3 mg/dL vs. 852.1 ± 48.5 mg/dL, $P = 0.81$), high-density lipoprotein cholesterol (Control vs. Linagliptin: before treatment, 6.7 ± 0.7 mg/dL vs. 6.4 ± 0.6 mg/dL, $P = 0.76$; at 16 weeks, 6.6 ± 0.5 mg/dL vs. 6.1 ± 0.4 mg/dL, $P = 0.51$), and triglycerides (Control vs. Linagliptin: before treatment, 194.9 ± 46.9 mg/dL vs. 217.4 ± 51.7 mg/dL, $P = 0.75$; at 16 weeks, 181.7 ± 30.1 mg/dL vs. 284.3 ± 42.2 mg/dL, $P = 0.07$). Casual blood glucose was also comparable between the control group and linagliptin group at baseline and after 16 weeks of treatment (Control vs. Linagliptin: before treatment, 183.1 ± 11.7 mg/dL vs. 171.0 ± 5.6 mg/dL, $P = 0.37$; at 16 weeks, 192.4 ± 16.5 mg/dL vs. 176.3 ± 11.8 mg/dL, $P = 0.44$).

iMAP-IVUS findings

The brachiocephalic artery was observed by iMAP-IVUS in the control group and the linagliptin group. Data obtained by iMAP-IVUS are shown in Tables 2 and 3, as well as Figs. 1

Table 1 Body weight and laboratory data before treatment and after 16 weeks in the two groups

	Baseline			16 weeks		
	Control (n = 8)	Linagliptin (n = 8)	P value	Control (n = 8)	Linagliptin (n = 8)	P value
BW (kg)	2.82 ± 0.08	2.84 ± 0.04	0.81	2.74 ± 0.11	3.00 ± 0.06	0.06
Total cholesterol (mg/dL)	1084.3 ± 75.5	1081.4 ± 83.4	0.98	938.9 ± 50.1	938.6 ± 42.0	0.99
LDL cholesterol (mg/dL)	1006.4 ± 73.8	991.4 ± 74.1	0.89	870.7 ± 57.3	852.1 ± 48.5	0.81
HDL cholesterol (mg/dL)	6.7 ± 0.7	6.4 ± 0.6	0.76	6.6 ± 0.5	6.1 ± 0.4	0.51
TG (mg/dL)	194.9 ± 46.9	217.4 ± 51.7	0.75	181.7 ± 30.1	284.3 ± 42.2	0.07
PG (mg/dL)	183.1 ± 11.7	171.0 ± 5.6	0.37	192.4 ± 16.5	176.3 ± 11.8	0.44
BUN (mg/dL)	17.4 ± 0.8	15.7 ± 1.2	0.26	18.3 ± 0.4	16.8 ± 1.4	0.34
Creatinine (mg/dL)	1.03 ± 0.06	0.93 ± 0.06	0.30	0.97 ± 0.04	0.94 ± 0.07	0.69
AST (U/L)	21.3 ± 2.9	21.7 ± 2.1	0.91	22.4 ± 2.0	26.0 ± 4.9	0.51
ALT (U/L)	44.9 ± 4.6	47.9 ± 4.5	0.65	43.0 ± 2.4	42.3 ± 3.8	0.88
LDH (U/L)	78.3 ± 20.0	64.7 ± 10.7	0.56	121.5 ± 33.8	105.0 ± 19.5	0.62
Na (mmol/L)	142.1 ± 0.6	141.7 ± 0.8	0.68	142.3 ± 0.6	142.4 ± 0.7	0.88
K (mmol/L)	3.0 ± 0.1	3.2 ± 0.2	0.44	3.0 ± 0.2	3.0 ± 0.1	0.91
Cl (mmol/L)	107.0 ± 0.8	104.0 ± 2.1	0.20	107.6 ± 1.8	106.0 ± 1.6	0.52

Data are shown as the mean ± SE

BW body weight, LDL low-density lipoprotein, HDL high-density lipoprotein, TG triglycerides, PG plasma glucose, BUN blood urea nitrogen, AST aspartate aminotransferase, ALT alanine aminotransferase, LDH lactic dehydrogenase, SE standard error

Table 2 iMAP-IVUS findings before treatment and at 16 weeks in the two groups

	Baseline			16 weeks		
	Control (n = 8)	Linagliptin (n = 8)	P value	Control (n = 8)	Linagliptin (n = 8)	P value
Vessel volume (mm ³)	45.84 ± 4.31	49.97 ± 2.55	0.42	44.61 ± 3.67	40.65 ± 3.03	0.42
Lumen volume (mm ³)	24.89 ± 3.36	27.18 ± 2.12	0.57	22.65 ± 2.76	21.56 ± 2.65	0.78
Plaque volume (mm ³)	20.94 ± 1.60	22.78 ± 1.64	0.43	21.96 ± 1.38	19.09 ± 1.20	0.14
%Plaque volume	46.34 ± 2.66	45.73 ± 2.45	0.15	50.06 ± 2.75	47.81 ± 2.84	0.25
Fibrotic volume (mm ³)	17.28 ± 1.90	19.56 ± 1.40	0.35	17.84 ± 0.96	14.05 ± 0.87	0.01
Lipidic volume (mm ³)	1.31 ± 0.12	1.50 ± 0.22	0.45	1.54 ± 0.22	1.03 ± 0.16	0.08
Necrotic volume (mm ³)	2.01 ± 0.28	2.74 ± 0.52	0.24	2.73 ± 0.49	1.85 ± 0.38	0.18
Calcified volume (mm ³)	0.12 ± 0.03	0.25 ± 0.08	0.17	0.24 ± 0.09	0.20 ± 0.05	0.96
Lipidic + necrotic volume (mm ³)	3.32 ± 0.37	4.24 ± 0.73	0.28	4.27 ± 0.68	2.87 ± 0.54	0.13
%Fibrotic	82.75 ± 3.22	82.00 ± 2.51	0.85	80.86 ± 2.81	82.00 ± 3.27	0.79
%Lipidic	6.25 ± 0.80	6.13 ± 0.79	0.91	6.50 ± 0.87	5.75 ± 1.00	0.57
%Necrotic	10.25 ± 2.52	11.25 ± 1.90	0.75	11.75 ± 1.94	10.75 ± 2.18	0.73
%Calcified	0.63 ± 0.18	1.13 ± 0.44	0.31	1.13 ± 0.44	0.88 ± 0.30	0.64
%Necrotic + lipidic	16.5 ± 3.22	17.38 ± 2.60	0.84	18.35 ± 2.63	16.50 ± 3.13	0.68

Data are shown as the mean ± SE

iMAP-IVUS iMap™ intravascular ultrasound, SE standard error

and 2. There were no significant differences in baseline vessel volume, plaque volume, lumen volume, and %plaque volume between the two groups, and no significant differences were found even after 16 weeks. For plaque composition, there were no significant differences in %fibrotic volume, lipidic plaque volume & %lipidic volume, necrotic plaque volume & %necrotic volume, and calcified plaque volume & %calcified volume between 2 groups in baseline and after

16 weeks treatment, except fibrotic volume was smaller in the linagliptin group after 16 weeks of treatment (Table 2).

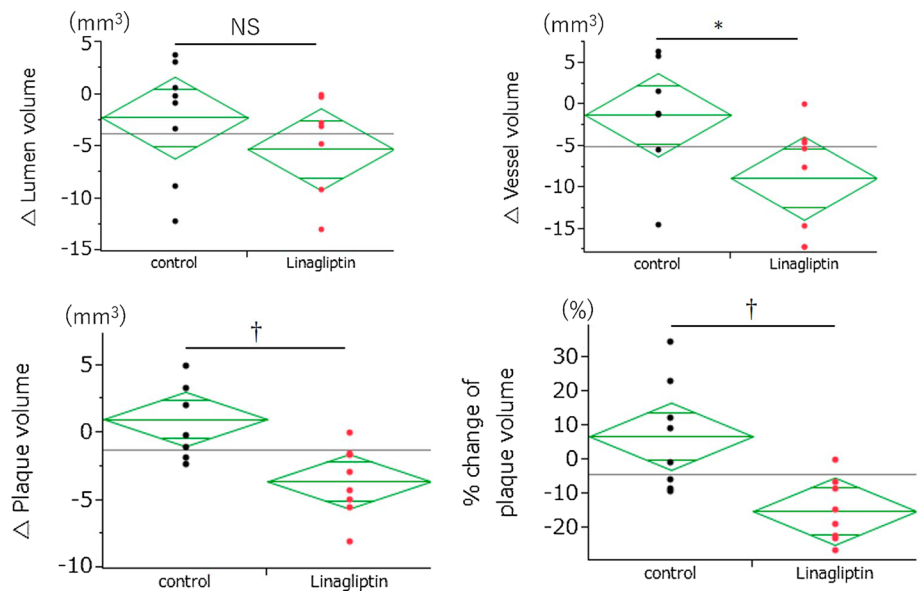
Comparison of changes in each parameter over 16 weeks of treatment between the two groups shows no significant difference in Δ lumen volume, but Δ vessel volume and Δ plaque volume decreased significantly in the linagliptin group (Table 3). While Δ %plaque volume did not show a significant difference between the two groups, the %change

Table 3 Changes in iMAP-IVUS findings from baseline to 16 weeks

	Control (<i>n</i> =8) 16 weeks – baseline	Linagliptin (<i>n</i> =8) 16 weeks – baseline	<i>P</i> value
ΔVessel volume (mm ³)	-1.22±2.36	-8.66±2.33	0.04
ΔLumen volume (mm ³)	-2.24±1.99	-5.27±1.66	0.26
ΔPlaque volume (mm ³)	1.02±0.96	-3.59±0.92	<0.01
Δ%Plaque volume	3.72±2.30	2.04±1.65	0.56
%change in plaque volume	6.90±5.62	-15.06±3.29	<0.01
ΔFibrotic volume (mm ³)	0.56±1.27	-5.57±1.46	0.04
ΔLipidic volume (mm ³)	0.24±0.24	-0.42±0.16	0.04
ΔNecrotic volume (mm ³)	0.76±0.54	-0.84±0.25	0.02
ΔCalcified volume (mm ³)	0.13±0.08	-0.08±0.11	0.14
ΔLipidic + necrotic volume (mm ³)	1.00±0.75	-1.26±0.38	0.02

Data are presented as the mean ± SE
SE standard error

Fig. 1 Changes in iMAP-IVUS parameters from baseline after 16 weeks in the control group and the linagliptin group. iMAP-IVUS iMap™ intravascular ultrasound, NS not significant, **P*<0.05, †*P*<0.01



in plaque volume (Δ plaque volume/baseline plaque volume $\times 100$, which compares the absolute change in plaque volume between the two groups) displayed a significant decrease in the linagliptin group (Table 3 and Fig. 1). The changes in plaque component are shown in Fig. 2. Δ fibrotic volume, Δ lipidic volume, and Δ necrotic volume were significantly decreased in the linagliptin group compared with the control group [Δ fibrotic volume: 0.56 ± 1.27 mm³ vs. -5.57 ± 1.46 mm³ (*P*=0.04), Δ lipidic volume: 0.24 ± 0.24 mm³ vs. -0.42 ± 0.16 mm³ (*P*=0.04), and Δ necrotic volume: 0.76 ± 0.54 mm³ vs. -0.84 ± 0.25 mm³ (*P*=0.02)].

Histopathology

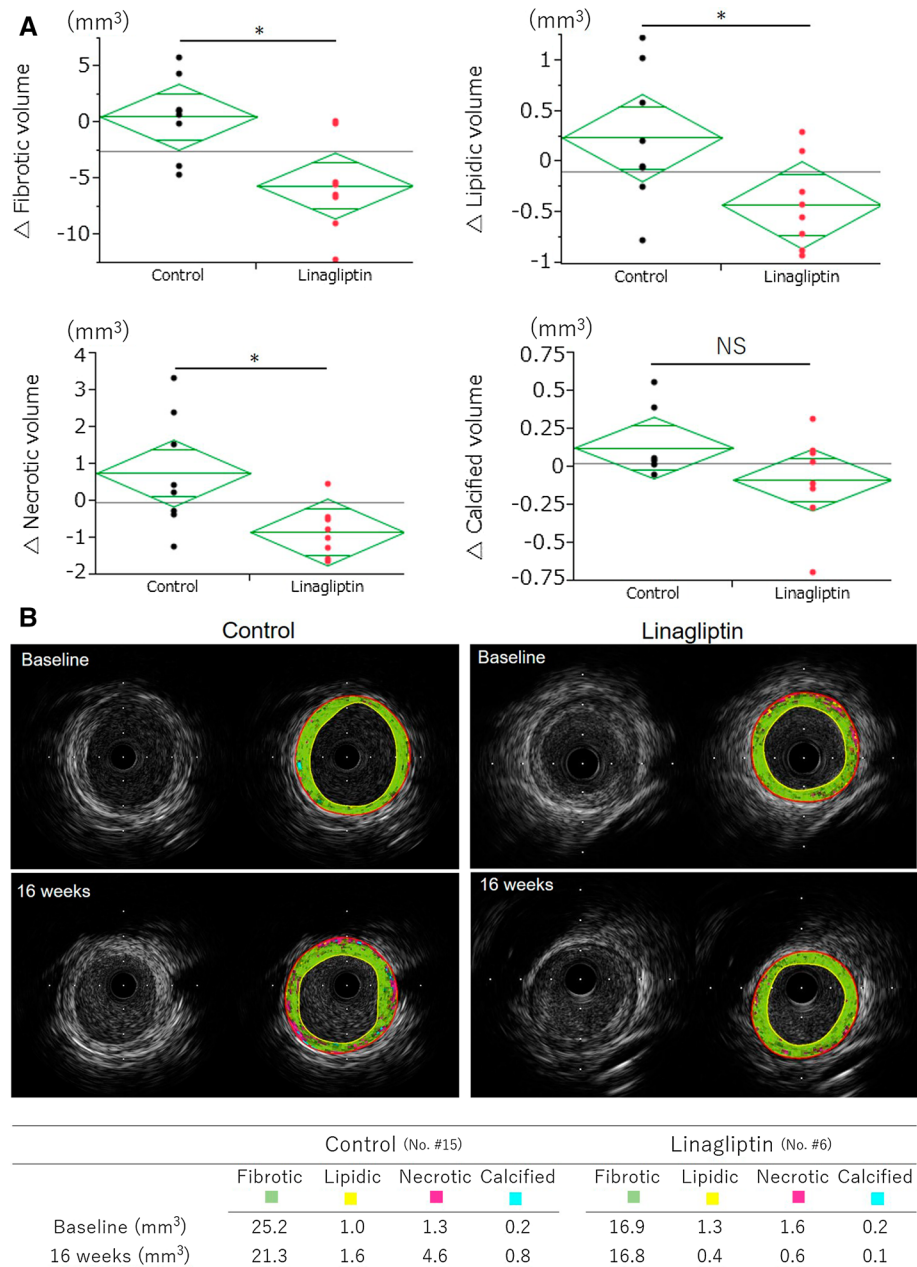
Pathologic findings are shown in Table 4 and Fig. 3. Corresponding to the IVUS data, there were no differences

between the two groups regarding to the vessel area, lumen area, intima area, media area, intima + media area, and %intima + media area (Table 4). Compared to control group, plaque macrophage infiltration was significantly reduced after 16 weeks of linagliptin treatment (Fig. 3a). The %SMC area, %fibrotic area, and calcification were comparable between the two groups (Fig. 3b–d).

Discussion

In this study, WHHL-MI rabbits were administered linagliptin or the vehicle for 16 weeks, and atherosclerotic lesions in the brachiocephalic artery were compared before and after administration by IVUS and pathological examination. We found that the administration of linagliptin suppressed the increase in plaque volume and %change in plaque volume

Fig. 2 iMAP-IVUS changes in plaque composition. Comparison of changes in fibrotic, lipidic, necrotic, and calcified volume after linagliptin treatments (a). Representative iMAP-IVUS images (No. #15 in control group, No. #6 in linagliptin group) at baseline and 16 weeks (b) NS not significant, * $P < 0.05$



compared with the control group. After 16 weeks, the linagliptin group showed no significant difference in lumen volume compared to the control group, but plaque volume and vessel volume were both decreased. In addition, infiltration of macrophages, the key player in plaque stability, was less prominent in the linagliptin group than in the control group. These findings suggested that progression of atherosclerotic plaque was inhibited, and plaque was stabilized by administration of linagliptin.

In mice, DPP-4 inhibitors have already been reported to improve vascular endothelial function, reduce atherosclerotic plaque, and reduce infiltration of macrophages into plaque [16, 17]. In addition, it has been reported that

DPP-4 inhibitors show anti-inflammatory activity in animal models of various inflammatory conditions, including colitis, asthma, and rheumatoid arthritis [18–20]. Furthermore, administration of linagliptin to rats with sepsis has been shown to suppress infiltration of CD11b- and CD11c-positive cells into the vascular wall, reduce oxidative stress, improve vascular endothelial function, and decrease vessel wall adhesion by monocyte and granulocytes [8]. Thus, DPP-4 inhibitors show anti-inflammatory effects in animal models of severe inflammatory conditions that can lead to atherosclerosis. Steven et al. [21] administered linagliptin to rats with lipopolysaccharide-induced sepsis and evaluated gene expression in the aortic wall by the quantitative

Table 4 Histological findings at 16 weeks

	Control (n=8)	Linagliptin (n=8)	P value
Vessel area (mm ²)	6.83 ± 0.73	8.29 ± 0.72	0.18
Lumen area (mm ²)	1.91 ± 0.37	2.46 ± 0.35	0.3
Intima area (mm ²)	3.73 ± 0.35	4.53 ± 0.35	0.14
Media area (mm ²)	1.17 ± 0.07	1.30 ± 0.08	0.28
Intima/media ratio	3.22 ± 0.24	3.51 ± 0.25	0.41
Intima + media (mm ²)	4.92 ± 0.39	5.83 ± 0.40	0.13
%Intima + media area (%)	73.11 ± 2.12	71.32 ± 2.14	0.12
%Macrophage area	12.03 ± 1.51	7.21 ± 1.65	<0.05
%SMC area	6.49 ± 0.73	6.24 ± 1.63	0.89
%Fibrotic area	53.60 ± 5.18	62.68 ± 6.44	0.29
%Calcified area	0.89 ± 0.25	1.06 ± 0.22	0.6

Data are presented as the mean ± SE. %Intima-media area = (intima area + media area)/vessel area × 100

SMC smooth muscle cell, SE standard error

real-time polymerase chain reaction, revealing downregulation of IL-6, VCAM-1, ICAM-1, MCP-1, CCL-2, and TNF- α expression in linagliptin-treated rats compared to control rats without an increase in inducible nitric oxide synthase expression. Therefore, this DPP-4 inhibitor has anti-inflammatory activity that may prevent progression of atherosclerosis.

In our previous study, another incretin-related drug, GLP-1 receptor agonist lixisenatide was administered to WHHL-MI rabbits for 12 weeks [22]. iMAP-IVUS analysis revealed that GLP-1 receptor agonist inhibited plaque growth and modified plaque composition with larger fibrotic plaque components and smaller necrotic and calcified plaque components in the GLP-1 group than in the control group. Histological analysis confirmed that GLP-1 receptor agonist treatment improved smooth muscle cell-rich plaque with increased fibrotic content. Furthermore, plaque macrophage infiltration and calcification were significantly reduced by GLP-1 receptor agonist treatment. Like lixisenatide, linagliptin also inhibited plaque growth and promoted plaque stabilization by inhibiting macrophage infiltration. These results highlight the theory that GLP-1 affect atherosclerosis through an anti-inflammatory mechanism. We also verified the correlation between IVUS and histopathological features in our previous study [22]. All values measured by iMAP-IVUS correlated clearly with the corresponding values measured histologically.

There were some limitations of this study. Acoustic shadowing interferes with the accuracy of detecting calcification by IVUS and impairs quantitative determination of tissue components behind calcified tissue. However, this factor may have had little impact in the present study, because calcification was not found in the surface layer of plaque, but in the deeper layers. The size of rabbit coronary arteries is too

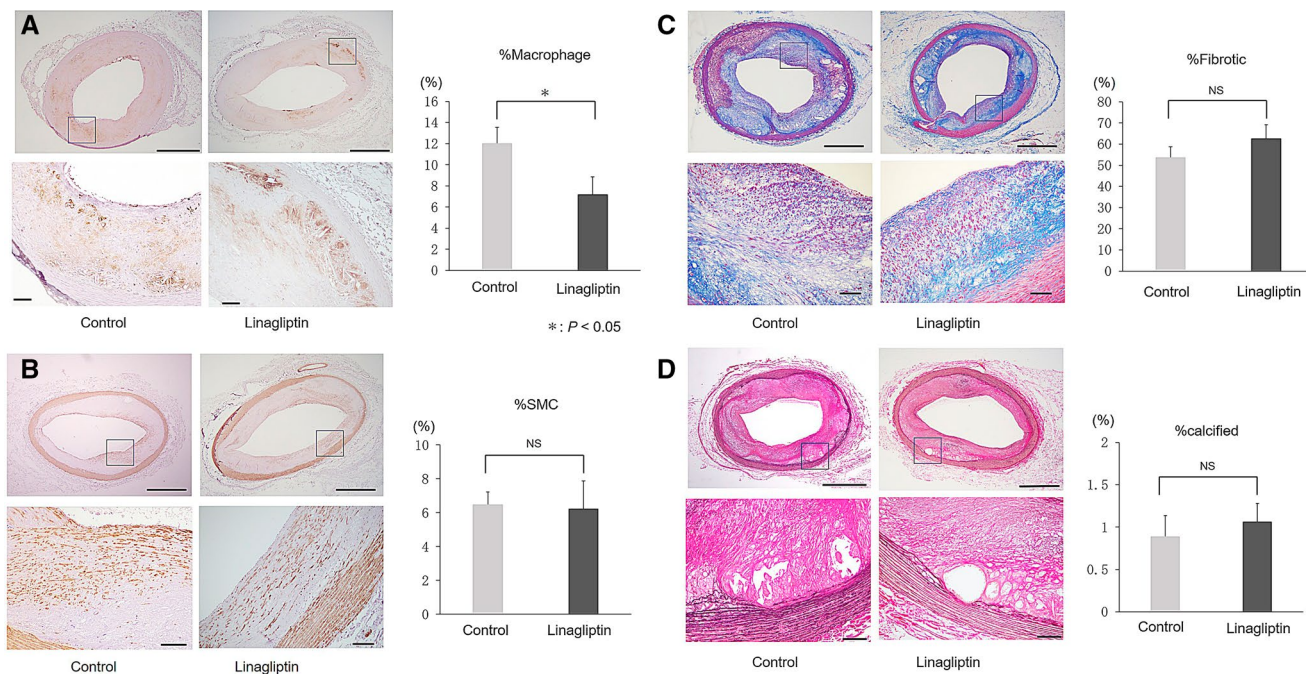


Fig. 3 Histological findings: Immunostaining of macrophages (a), immunostaining of smooth muscle α actin (b), Masson Trichrome staining (c), and EVG staining (d). * $P < 0.05$: control group vs. linagliptin group

Upper panels: scale bar shows 1 mm. Lower panels: scale bar shows 100 μ m. EVG Elastica van Gieson, SMC smooth muscle cell

small to be observed by intravascular imaging, and the rabbit aorta is larger than human coronary arteries and difficult to be imaged by IVUS. Hence, we selected the brachiocephalic artery as a substitute, which diameter is close to the diameter of human coronary arteries. However, since the vessel structure and hemodynamics are different, the state of the plaque and the processes of its development may not have been the same as in the coronary arteries. Like IVUS, optical coherence tomography (OCT) is another intravascular imaging proved to be more sensitive to identify macrophages. We tried to capture OCT images in WHHL-MI rabbits in our preliminary experiments. However, all rabbits died soon after the OCT procedure. We suspect that rabbit is too small to bear the human dose contrast injection through guiding catheter to remove blood from brachiocephalic artery, which is necessary to obtain OCT images. The cause of death might be contrast-induced cerebrovascular hypertension and brain tissue edema.

Conclusion

Linagliptin treatment might suppress progression of plaque volume and contribute to the stabilization of plaque. Linagliptin showed both anti-inflammatory and anti-atherosclerotic effects in WHHL-MI rabbits with chronic inflammatory atherosclerosis.

Acknowledgements We thank the staff at the Nihon University Medical Research Support Center for their assistance with animal management. We offer special thanks to Rie Takahashi and Yoshiki Taniguchi for their excellent technical assistance.

Compliance with ethical standards

Conflict of interest The authors declare that they have no conflict of interest.

Statement on the welfare of animals The experimental protocol was approved by the Animal Care and Use Committee of Nihon University (No. AP15M012). All procedures performed in studies involving animals were in accordance with the ethical standards of the institution.

References

- UK Prospective Diabetes Study (UKPDS) Group (1998) Intensive blood-glucose control with sulphonylureas or insulin compared with conventional treatment and risk of complications in patients with type 2 diabetes (UKPDS 33). *Lancet* 352(9131):837–853
- ACCORD Study Group; ACCORD Eye Study Group, Chew EY, Ambrosius WT, Davis MD, Danis RP, Gangaputra S, Greven CM, Hubbard L, Esser BA, Lovato JF, Perdue LH, Goff DC Jr, Cushman WC, Ginsberg HN, Elam MB, Genuth S, Gerstein HC, Schubarth U, Fine LJ (2010) Effects of medical therapies on retinopathy progression in type 2 diabetes. *N Engl J Med* 363(3):233–244
- Nathan DM, Buse JB, Davidson MB, Ferrannini E, Holman RR, Sherwin R, Zinman B (2009) Medical management of hyperglycemia in type 2 diabetes: a consensus algorithm for the initiation and adjustment of therapy: a consensus statement of the American Diabetes Association and the European Association for the Study of Diabetes. *Diabetes Care* 32(1):193–203
- Anderson RJ, Bahn GD, Moritz TE, Kaufman D, Abaira C, Duckworth W; VADT Study Group (2011) Blood pressure and cardiovascular disease risk in the veterans affairs diabetes trial. *Diabetes Care* 34(1):34–38
- Zhong J, Kankanala S, Rajagopalan S (2016) Dipeptidyl peptidase-4 inhibition: insights from the bench and recent clinical studies. *Curr Opin Lipidol* 27(5):484–492
- Stocker R, Keaney JF Jr (2004) Role of oxidative modifications in atherosclerosis. *Physiol Rev* 84(4):1381–1478
- Mizuno Y, Jacob RF, Mason RP (2011) Inflammation and the development of atherosclerosis. *J Atheroscler Thromb* 18(5):351–358
- Kroller-Schon S, Knorr M, Hausding M, Oelze M, Schuff A, Schell R, Sudowe S, Scholz A, Daub S, Karbach S, Kossmann S, Gori T, Wenzel P, Schulz E, Grabbe S, Klein T, Münzel T, Daiber A (2012) Glucose-independent improvement of vascular dysfunction in experimental sepsis by dipeptidyl-peptidase 4 inhibition. *Cardiovasc Res* 96(1):140–149
- Shiomi M, Ito T, Yamada S, Kawashima S, Fan J (2003) Development of an animal model for spontaneous myocardial infarction (WHHLM rabbit). *Arterioscler Thromb Vasc Biol* 23(7):1239–1244
- Nicholls SJ, Ballantyne CM, Barter PJ, Chapman MJ, Erbel RM, Libby P, Raichlen JS, Uno K, Borgman M, Wolski K, Nissen SE (2011) Effect of two intensive statin regimens on progression of coronary disease. *N Engl J Med* 365(22):2078–2087
- Sathyanarayana S, Carlier S, Li W, Thomas L (2009) Characterisation of atherosclerotic plaque by spectral similarity of radiofrequency intravascular ultrasound signals. *EuroIntervention* 5(1):133–139
- Araki T, Nakamura M, Utsunomiya M, Sugi K (2012) Visualization of coronary plaque in type 2 diabetes mellitus patients using a new 40 MHz intravascular ultrasound imaging system. *J Cardiol* 59(1):42–49
- Garcia-Garcia HM, Gogas BD, Serruys PW, Bruining N (2011) IVUS-based imaging modalities for tissue characterization: similarities and differences. *Int J Cardiovasc Imaging* 27(2):215–224
- Lin QF, Luo YK, Zhao ZW, Cai W, Zhen XC, Chen LL (2013) Atherosclerotic plaque identification by virtual histology intravascular ultrasound in a rabbit abdominal aorta model of vulnerable plaque. *Exp Biol Med (Maywood)* 238(11):1223–1232
- Fukuda K, Iihara K, Maruyama D, Yamada N, Ishibashi-Ueda H (2014) Relationship between carotid artery remodeling and plaque vulnerability with T1-weighted magnetic resonance imaging. *J Stroke Cerebrovasc Dis* 23(6):1462–1470
- Matsubara J, Sugiyama S, Sugamura K, Nakamura T, Fujiwara Y, Akiyama E, Kurokawa H, Nozaki T, Ohba K, Konishi M, Maeda H, Izumiya Y, Kaikita K, Sumida H, Jinnouchi H, Matsui K, Kim-Mitsuyama S, Takeya M, Ogawa H (2012) A dipeptidyl peptidase-4 inhibitor, des-fluoro-sitagliptin, improves endothelial function and reduces atherosclerotic lesion formation in apolipoprotein E-deficient mice. *J Am Coll Cardiol* 59(3):265–276
- Shah Z, Kampfrath T, Deiuliis JA, Zhong J, Pineda C, Ying Z, Xu X, Lu B, Moffatt-Bruce S, Durairaj R, Sun Q, Mihai G, Maisey A, Rajagopalan S (2011) Long-term dipeptidyl-peptidase 4 inhibition reduces atherosclerosis and inflammation via effects on monocyte recruitment and chemotaxis. *Circulation* 124(21):2338–2349
- Iwaya H, Fujii N, Hagio M, Hara H, Ishizuka S (2013) Contribution of dipeptidyl peptidase IV to the severity of dextran sulfate

- sodium-induced colitis in the early phase. *Biosci Biotechnol Biochem* 77(7):1461–1466
19. Schade J, Schmiedl A, Kehlen A, Veres TZ, Stephan M, Pabst R, von Horsten S (2009) Airway-specific recruitment of T cells is reduced in a CD26-deficient F344 rat substrain. *Clin Exp Immunol* 158(1):133–142
 20. Busso N, Wagtmann N, Herling C, Chobaz-Peclat V, Bischof-Delaloye A, So A, Grouzmann E (2005) Circulating CD26 is negatively associated with inflammation in human and experimental arthritis. *Am J Pathol* 166(2):433–442
 21. Steven S, Hausding M, Kroller-Schon S, Mader M, Mikhed Y, Stamm P, Zinssius E, Pfeffer A, Welschhof P, Agdauletova S, Sudowe S, Li H, Oelze M, Schulz E, Klein T, Munzel T, Daiber A (2015) Gliptin and GLP-1 analog treatment improves survival and vascular inflammation/dysfunction in animals with lipopolysaccharide-induced endotoxemia. *Basic Res Cardiol* 110(2):6
 22. Sudo M, Li Y, Hiro T, Takayama T, Mitsumata M, Shiomi M, Sugitani M, Matsumoto T, Hao H, Hirayama A (2017) Inhibition of plaque progression and promotion of plaque stability by glucagon-like peptide-1 receptor agonist: serial in vivo findings from iMap-IVUS in Watanabe heritable hyperlipidemic rabbits. *Atherosclerosis* 265:283–291

Publisher's Note Springer Nature remains neutral with regard to jurisdictional claims in published maps and institutional affiliations.